Nuclear Instruments and Methods in Physics Research A 762 (2014) 130–134

Contents lists available at ScienceDirect

Nuclear Instruments and Methods in Physics Research A

journal homepage: www.elsevier.com/locate/nima

Thermal neutron response and theoretical comparison of LiF coated aluminized Mylar

Kyle A. Nelson *, Steven L. Bellinger, Nathaniel S. Edwards, Benjamin W. Montag, Aaron J. Schmidt, Clayton Wayant, Douglas S. McGregor

S.M.A.R.T. Laboratory, Mechanical and Nuclear Engineering, Kansas State University, Manhattan, KS 66506, USA

ARTICLE INFO

Article history:
Received 14 October 2013
Received in revised form
3 April 2014
Accepted 6 May 2014
Available online 27 May 2014

Keywords:
Neutron detector
Proportional counter
LiF coated Mylar

ABSTRACT

Thin layers of LiF were deposited on a 2.0 μm thick aluminized BoPET (i.e. Mylar) in thicknesses of 4.5, 9.9, and 14.0 μm using an electron beam evaporator. These coatings were thinner than the summed triton and alpha particle range from the ^{6}Li(n,t)^{4}He reaction, which allows both particles to escape a suspended absorber sheet simultaneously and measured in a proportional gas region concurrently. Each thickness of the LiF coated Mylar sheets were positioned separately in a test chamber that had a single anode wire positioned on each side of the absorber sheets. The thermal neutron response pulse-height spectra were collected for each LiF thickness and are presented and discussed. The coatings became fragile at thicknesses greater than 5.0 μm and would flake off of the Mylar sheets. Additionally, the ideal LiF coating thickness that maximizes the intrinsic thermal neutron detection efficiency is greater than 5.0 μm, which is discussed in a greater detail in the text. Overall, the detectors are capable of achieving thermal-neutron detection efficiencies greater than 30% for a 5 layer device and 60 % for 20 layers, but these devices are complex to fabricate due to flaking of the LiF coatings. Additional research is required to eliminate flaking by possibly using additional mechanical structures or adhesive materials.

1. Introduction

The ability of a gas-filled neutron detector to measure more than one reaction product per neutron absorption from a solid-form neutron absorber has been utilized to study different types of ^{3}He neutron detector alternatives [1,2]. These new detector types typically use thin neutron absorber sheets, such as Li foil, but can also be demonstrated using high-porosity, low-density materials [3,4]. Ideally, the ^{6}Li(n,t)^{4}He and ^{10}B(n,α)^{7}Li reactions are utilized because of their large neutron-absorption cross-sections and relatively short range energetic reaction products. The ability to measure both reaction-products per neutron absorption increases both the overall neutron detection efficiency and the gamma-ray discrimination quality of a detector.

Conventional gas-filled neutron detectors using a solid-form neutron absorber measure only one reaction-product per neutron absorption. The most common type of detector fitting this description is the ^{10}B-lined proportional counter, in which one reaction product escapes the boron coating and enters the gas region of the detector. For thermal-neutron absorptions (0.025 eV), however, the other reaction product ejects in the opposite direction towards the cathode chamber wall and does not deposit energy in the gas region [5]. The reaction product that does enter the gas volume may have significant energy loss through self-absorption as the particle traverses the neutron absorber coating layer before reaching the gas region. Consequently, the pulse-height spectrum of ^{10}B-lined tubes contains multiple steps that blend into the lower portions of the pulse-height spectrum where electronic noise and pulses from gamma-ray interactions typically reside, a spectral feature referred to as the 'wall effect' [6].

The thin neutron absorber medium demonstrated here uses LiF as the neutron reactive material, and thus utilizes the ^{6}Li(n,t)^{4}He reaction. The microscopic thermal-neutron absorption cross-section for ^{6}Li is 940 b and has a natural abundance of 7.59% [6]. Enriched ^{6}LiF has a density of 2.54 g/cm^{3} and a macroscopic thermal neutron absorption cross section of 57.51 cm^{-1}. The ^{6}Li(n,t)^{4}He reaction leads to the following products, with a total reaction *Q*-value of 4.78 MeV [7]

$$^{6}\mathrm{Li} + {}^{1}_{0}\mathrm{n} \rightarrow {}^{3}\mathrm{H}(2.73\ \mathrm{MeV}) + \alpha(2.05\ \mathrm{MeV}).$$

There are several neutron-absorber materials that can be suspended between proportional counter regions including Li foil, impregnated foam, and aerogels, all which are currently being investigated [3,4]. Boron, although categorized as a metal, cannot be rolled into typical foils similar to aluminum or lithium. However, boron and boron compounds can be evaporated onto thin

* Corresponding author.
E-mail address: knelson1@ksu.edu (K.A. Nelson).

http://dx.doi.org/10.1016/j.nima.2014.05.077
0168-9002/

membranes such as biaxially-oriented polyethylene terephthalate (BoPET), trademarked as Mylar, but the summed coating and substrate thickness must be less than the summed range of the reaction products in order to avoid the wall-effect. The reaction product ranges from the $^{10}B(n,\alpha)^{7}Li$ reaction,

$$^{10}B + {}^{1}_{0}n \rightarrow \alpha(1.47\ \text{MeV}) + {}^{7}Li(0.84\ \text{MeV}) + \gamma(0.48\ \text{MeV}) \quad 94\%$$

$$^{10}B + {}^{1}_{0}n \rightarrow \alpha(1.78\ \text{MeV}) + {}^{7}Li(1.02\ \text{MeV}) \quad 6\%$$

are relatively short compared to the ranges of the reaction products from the $^{6}Li(n,t)^{4}He$ reaction [7]. Thus, evaporation deposition can also be performed with Li based compounds, such as LiF. The ranges of the triton and alpha particle are long compared to the boron reaction product ranges, thereby, allowing for a thickness of the LiF coating to be up to several tens of microns thick with negligible wall-effect.

Herein reported are the details of the design, performance, and theoretical comparison of LiF coated aluminized Mylar neutron absorber sheets. Specifically, LiF was evaporated onto Mylar at different thicknesses and thermal-neutron response pulse-height spectra were collected and compared to MCNP6 simulated results. Further, theoretical calculations were performed to determine the ideal LiF thickness that would maximize the intrinsic thermal-neutron detection efficiency for various layers of LiF neutron absorber sheets. This work was first presented at the IEEE Symposium on Radiation Measurements and Applications (SORMA) in May 2012. Similar research was completed in parallel by another organization, but focuses on different aspects of the technology [8].

2. Theoretical considerations

Shown in Fig. 1 is a cross-sectional schematic of LiF coated aluminized Mylar. The thicknesses reported in Fig. 1 are less than the summed range of the reaction products from the $^{6}Li(n,t)^{4}He$ reaction. The ranges of the triton and alpha particle in pure ^{6}LiF are 33.6 μm and 6.05 μm, respectively; hence, the summed range is 39.65 μm [9]. The Mylar substrate can absorb a portion of the reaction product energy before it reaches the proportional gas volume. Minimum energy loss of the alpha particle and triton reaction products when they traverse the Mylar before entering the gas volume is 440 keV and 70 keV, respectively [9]. Differences in energy loss between the alpha particle and triton are a result of the stopping power(s) being greater for the alpha particle than for the triton, described by the Bethe–Bloch stopping power formula [5–7]. It should also be noted that the aluminum coating on the Mylar is thin (< 0.05 μm) enough to be considered negligible in the cases described here.

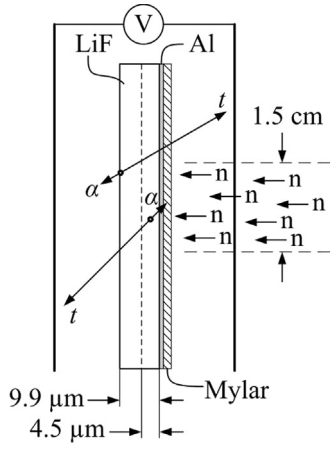

Fig. 1. A cross-sectional schematic of the LiF coated Mylar showing two different thicknesses of LiF coating. The reaction products are able to escape both sides of the absorber sheet simultaneously and be measured in separate gas compartments concurrently.

There are three reaction product combination paths that can result in a measurable event. The first occurs when both reaction products escape the absorber/Mylar and are measured simultaneously. The second occurs when only the triton escapes the absorber/Mylar sheet and the last occurs when only the alpha particle escapes and creates ionization in the gas. In the latter two occurrences, the unmeasured reaction product is absorbed by the LiF and/or Mylar, and thus does not contribute to signal generation. For the thicknesses investigated here, the probability that the induced signal is resultant only from the triton contribution is the highest, followed by simultaneous contributions of both particles, and finally the lowest probability event being the response from only the alpha particle entering the gas volume. There is also a probability that neither reaction product escapes and no signal is generated, a probability that increases with increasing absorber thickness. After the reaction products enter the gas medium, they deposit their energy and generate free electron-ion pairs through Coulombic interactions. The electrons travel to the central anode wire under the applied electric-field where the device operates as a conventional proportional counter by creating a Townsend avalanche, while the associated positive ions drift towards the cathode wall.

The intrinsic thermal-neutron detection efficiency was calculated for various layers of pure ^{6}LiF foils as a function of the foil thickness and is shown in Fig. 2. The method used to obtain these values is described in great detail elsewhere [7], and uses an energy threshold, or lower level discriminator (LLD), of 300 keV while accounting for the attenuation of neutrons through successive foils. The calculations were performed for ^{6}LiF foils with no substrate because these values are the absolute highest detection efficiencies possible with LiF sheets completely independent of the substrate material and thickness. Substrates as thin as 1.0 nm may be possible, and as the substrate thickness decreases, the intrinsic thermal-neutron detection efficiency will approach the values shown in Fig. 2. The intrinsic thermal-neutron detection efficiency is maximized at a specific LiF thickness for a particular number of LiF foil layers, as shown in Fig. 2. For example, the ideal thickness for a set of 15 ^{6}LiF-foils ranges between 9 and 10 μm and has an intrinsic thermal neutron detection efficiency of 57%, while a five layer device has an efficiency of 32% with an optimized coating thickness of 14 μm. The extra 2.0 μm thick Mylar substrate will decrease the overall neutron detection efficiency while minimally changing the ideal thickness for a specific number set of layers. The Mylar will increase self-absorption of the reaction products

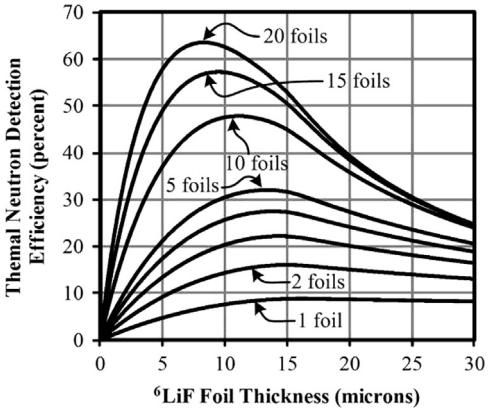

Fig. 2. The theoretical intrinsic thermal-neutron detection efficiency of ^{6}LiF foils for various layers of absorber sheets as a function of ^{6}LiF foil thickness.

and reduce their escape probabilities because of the added thickness. Further, as the substrate material thickness increases, the ideal coating thickness and detection efficiency both decrease.

The theoretical thermal-neutron response pulse-height spectra obtained for LiF coating thicknesses of 0.1 μm, 4.5 μm, 9.9 μm, and 14.0 μm on 2.0 μm thick Mylar sheet were obtained using MCNP6 and are shown in Figs. 3 and 4. In the simulation, a uniformly distributed 1.5 cm diameter collimated thermal-neutron beam was centered on 15 cm × 15 cm ^{6}LiF coated aluminized Mylar sheet centered within an aluminum test chamber 15 × 15 × 15 cm^3 and filled with P-10 proportional gas (90% Ar, 10% CH_4). Centering the beam allows the entire energy of the triton to be absorbed in the gas without reaction products colliding with the Al cathode wall. The triton range in 1.0 atm of P-10 gas is 7.26 cm [9]. The neutron beam dimensions and energy were chosen to resemble the diffracted thermal-neutron beam at the Kansas State University (KSU) TRIGA Mark II nuclear reactor. Hence, a direct comparison can be made between the experimental LiF coated Mylar pulse-height spectra and the simulated data. An additional 0.1 μm thick ^{6}LiF coating pulse-height spectrum is included in Fig. 3 that serves to show the simulations are correct. The largest energy peak appears just below the reaction *Q*-value (4.78 MeV) at 4.71 MeV, which occurs when the triton traverses the Mylar before entering the P-10 gas and the alpha particle enters directly into the gas from a surface absorption. Additionally, there are peaks at each of the reaction product characteristic energies, which occur when only one reaction product is measured and the other is absorbed in the LiF and/or Mylar. Obviously, the alpha particle being absorbed in the LiF and Mylar occurs more frequently than the triton, thus accounting for the differences between peak heights in the spectrum. There is an additional feature at 4.34 MeV, 440 keV below the *Q*-value, which is the result of the triton immediately entering the P-10 gas region from a surface absorption and the alpha particle traversing the Mylar before entering the gas region.

The theoretical pulse-height spectra with the thicker ^{6}LiF coatings, shown in Fig. 4, show a sudden drop in counts at 2.73 MeV, the energy of the triton. Any pulses that occur above this value are from both reaction-products escaping the absorber simultaneously. These pulses decrease in frequency with increasing LiF coating thickness. Additionally, the width of the main feature in the pulse-height spectra, positioned between 1.5 MeV and 2.73 MeV, increases with increasing LiF coating thickness. The thicker coatings cause more self-absorption of the reaction products to occur before they escape the surface of the absorber assembly. However, each coating thickness simulated has a large valley appearing between the lowest energy region where gamma-rays and electronic noise might appear and the main feature of the pulse-height spectra. This valley is an important feature because it allows the user to set the LLD relatively high, thereby eliminating most gamma-ray induced pulses with minimal sacrifice of neutron generated events. Thus, the total thermal-neutron detection efficiency should remain relatively constant over a wide range of LLD settings compared to a device with a prominent wall-effect in the pulse-height spectrum.

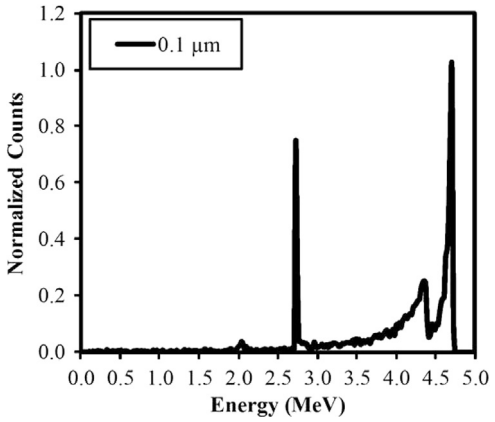

Fig. 3. The simulated thermal-neutron response pulse-height spectrum of a 0.1 μm thick LiF coating on 2.0 μm aluminized Mylar (obtained using MCNP6).

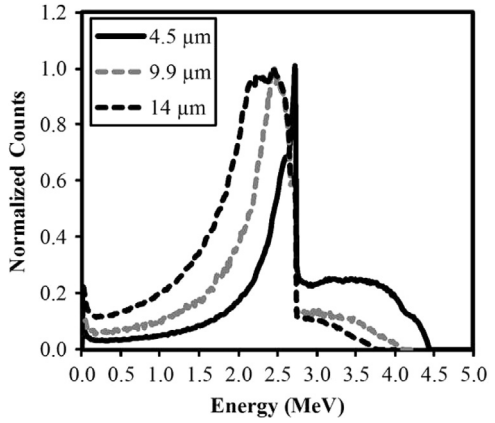

Fig. 4. The simulated thermal-neutron response pulse-height spectra of 4.5, 9.9, and 14.0 μm thick LiF coatings on 2.0 μm aluminized Mylar (obtained using MCNP6).

3. Experimental procedure

Aluminized Mylar, 2.0 μm thick, was stretched across 15 cm × 15 cm aluminum frames and taped to the edges using copper tape. The open area of the frames was 12.7 cm × 12.7 cm and the Mylar was stretched to a mirror smooth finish. Natural LiF was deposited on the aluminized side of the Mylar using an electron-beam evaporation system. The LiF adhered better to the aluminized side versus the bare Mylar side. Three frames were constructed and three rounds of the LiF evaporation process were conducted initially with all frames loaded into the evaporator. During each round, between 4 and 5 μm of LiF was deposited. At the end of each evaporation process one of the frames was removed. Thus, the final thicknesses of the LiF coatings were 4.5 μm, 9.9 μm, and 14.0 μm. The thicknesses were obtained from the electron-beam evaporation oscillating crystal monitor set for the density and *Z* ratio of LiF. At each film thickness, the LiF coated Mylar sheets were centered in an aluminum test chamber approximately 15 cm × 15 cm × 15 cm. The test chamber was purged with P-10 gas and positioned at the KSU TRIGA Mark II nuclear reactor diffracted thermal-neutron beam. The reactor power was increased to 100 kW and a 1.5 cm diameter neutron beam irradiated the center of the sheet. Two 10 min pulse-height spectra were collected: one with a Cd-shutter to block all incident thermal neutrons and another without the Cd-shutter. The pulse-height spectra were plotted with the simulated spectra results and are shown in the following section.

4. Experimental results

The thermal-neutron response pulse-height spectra obtained for the 4.5, 9.9, and 14.0 μm thick LiF coated aluminized Mylar sheets are shown in Figs. 5–7, respectively. Additionally, the theoretical pulse-height spectra of the absorber sheets obtained with MCNP6 are included in these figures. Each pulse-height spectra had the expected valley as previously described, but the electronic noise is apparent in the experimentally obtained spectra, as expected. The percentage of total counts with energy greater than 2.73 MeV decreases with

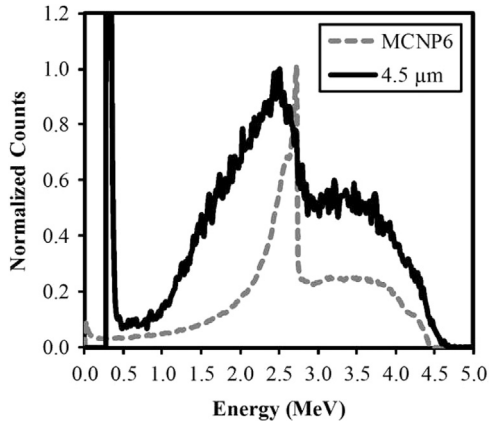

Fig. 5. The experimental and simulated (MCNP6) thermal-neutron response pulse-height spectra of 4.5 μm thick LiF coated aluminized Mylar.

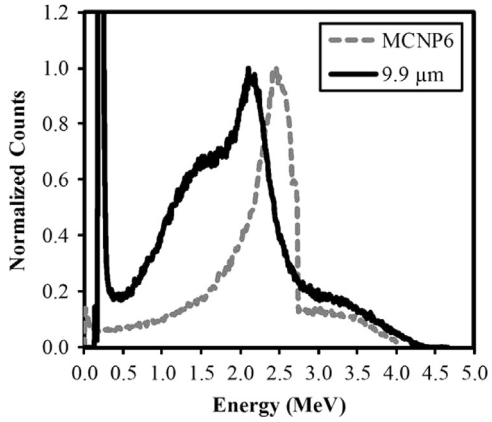

Fig. 6. The experimental and simulated (MCNP6) thermal-neutron response pulse-height spectra of 9.9 μm thick LiF coated aluminized Mylar.

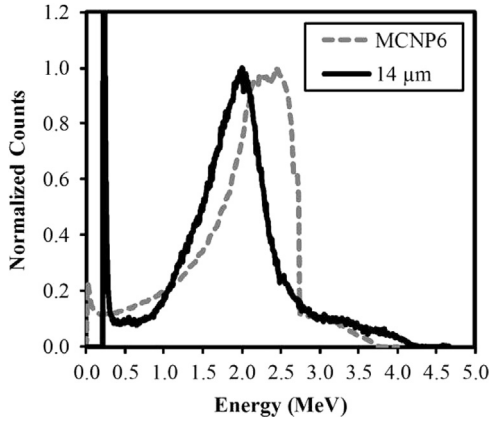

Fig. 7. The experimental and simulated (MCNP6) thermal-neutron response pulse-height spectra of 14 μm thick LiF coated aluminized Mylar.

increasing LiF coating thickness as predicted by the simulations. Natural LiF was used for the investigation, and, thus, no intrinsic thermal-neutron detection efficiency measurements or calculations were conducted.

5. Discussion

The spectral shapes of the different experimental pulse-height spectra do not exactly match the simulated spectra although the shapes are in general agreement. There are three main reasons for the discrepancies. First, and most likely, is the delamination of the LiF from the Mylar, which is discussed in greater detail in the following paragraph. Second, the MCNP6 model does not contain any code to simulate the electric field, charge migration, or resolution of the gas-filled detector. Thus, the sharp peaks in the simulation are not possible experimentally. Further, the electric field inside the square chamber is not uniform, thus, charge collection may also be non-uniform. At the furthest distance from the anode wire, 10.6 cm, the electric field may be weak and have a different charge collection efficiency than charges generated near the anode wire. Installing multiple anode wires on each side of the absorber sheet may have decreased this effect. Additionally, a square chamber is not ideal for obtaining a uniform electric field. Lastly, albedo neutrons from room scatter in the nuclear reactor bay can produce a substantial background source of incident neutrons, although significantly lower than the collimated neutron beam.

The normalized counts above 2.73 MeV of the experimental data match the simulated spectra well for the 9.9 μm and 14.0 μm thick coatings, which was not the case for the 4.5 μm thick spectra. It is not definitively conclusive why the 4.5 μm pulse-height spectra do not agree to the same level of accuracy as the other thicknesses. One feature that does agree with the simulation is the higher percentage of events above 2.73 MeV compared to the other coating thicknesses. The higher percentage is a result of the thinner coating, which allows for a high probability that both reaction products escape simultaneously. However, there could be some inaccuracies and inconsistencies to the coating thickness which caused the deviation of the experimental spectrum from the simulated. One possible cause for the irregularity could be parallax effects in the evaporator, but this was not investigated. Another indication of thickness variation is the delamination of sections of the LiF coating. The chances of material flaking-off increased rapidly with increasing coating thickness, and were observed on all samples with coatings greater than 5.0 μm. The flaking of one 9.9 μm thick LiF coated Mylar absorber layer is shown in Fig. 7 in the upper right quadrant of the sheet. It was also unclear if only a fraction of the total LiF coating thickness was detached. In other words, certain sections of the absorber sheet may have been thicker or thinner due to flaking. Note that the coated sample shown in Fig. 8 was exposed to open air for approximately 18 months and showed no further signs of degradation.

The pulse-height spectra show changes for both experimental and simulated data when using a collimated source versus an isotropic point source, and also when a collimated source is positioned closer to the cathode wall as opposed to the anodes. Reaction products born near the cathode wall may collide with the cathode wall, thereby, depositing only a fraction of its energy in the gas volume, consequently, producing smaller pulses. These smaller pulses would shift pulse-height features to lower energies, or channel numbers, and broaden the energy peaks as well. Further, as a result of the restricted reaction product ranges, the valley depth in the pulse-height spectra decreases. This shift in pulse-height spectra was investigated further using MCNP6 by shifting the distance of the collimated neutron beam from the center to the corner of the LiF sheet. Pulse-height spectra were simulated with the 1.0 cm diameter collimated beam center located 7.5 cm from each edge of the sheet and the center location to edge distance was changed to 4.2, 2.5, and 0.8 cm. Pulse-height spectra collected from these simulations are shown in Fig. 9, where the shift in spectral features is obvious and a result of the reaction products colliding with the cathode wall and depositing only a fraction of their total energy in the gas volume. Each simulation was completed using 4.0×10^7 histories, thus, the spectral shapes of each thickness are of proper proportionality to one another.

The feasibility of consistently producing repeatable results with these detectors is low due to the delamination of the LiF coating at thicknesses deemed less than ideal for maximizing the thermal neutron detection efficiency. LiF detachment was reduced when

Fig. 8. The aluminized Mylar sheet coated with 9.9 μm of LiF which shows the flaking of the LiF occurring in the top right quadrant of the pane.

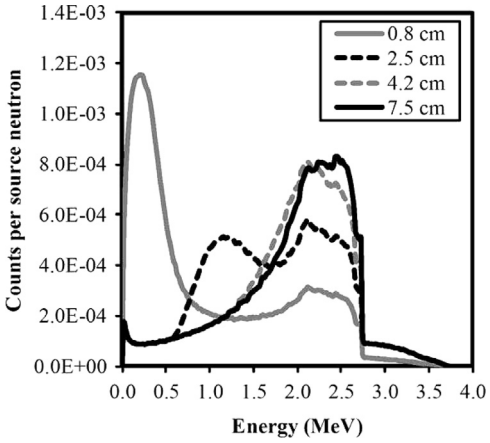

Fig. 9. The simulated thermal-neutron response pulse-height spectra of 14.0 μm thick LiF on 2.0 μm aluminized Mylar obtained using MCNP6 for beam center to sheet edge distances of 7.5, 4.2, 2.5, and 0.8 cm. Pulses decrease in size due to reaction products colliding with the cathode wall and depositing only a fraction of their energy, which results in more pulses in lower channel numbers.

the Mylar material was stretched to a mirror finish, yet, any vibration to the frame also caused the LiF to delaminate. Another cause for delamination may have been the thermal expansion and contraction of the Mylar due to temperature changes. Some options to decrease the amount of flaking are to spray a coating material on top of the LiF or to trap the LiF between additional Mylar. However, this coating process would only decrease the intrinsic neutron detection efficiency and possibly add more complications to the construction technique. Further, other materials could be used as a substrate including, Kapton tape and aluminum or copper foil, which may have better LiF adhesion.

6. Conclusions

Based on the results and observations presented here, the following can be stated:

1. Intrinsic thermal neutron detection efficiencies greater than 30% are possible with multiple ^{6}LiF coated Mylar sheets stacked together.
2. LiF can be coated on aluminized Mylar but will flake-off at thicknesses greater than 5 μm without an additional adhesive layer.
3. The suspended coated Mylar sheets have a pulse-height spectrum with a large valley separating the electronic noise from the main feature. This is an important feature to have and will result in good gamma-ray discrimination capabilities with minimal loss of neutron sensitivity.
4. The feasibility and fragility of the LiF coatings complicated device construction and compromised performance consistency, which would consequently affect the reliability and efficiency of the devices.
5. Additional physical structure or adhesive material must be included in future permutations of the detector in order to reduce the delamination of the LiF, which may be accomplished through a plurality of methods.

Acknowledgments

This work was supported in part by the U.S. Defense Threat Reduction Agency (DTRA), under contract HDTRA1-12-c-0002. The authors express their gratitude to the KSU TRIGA Mark II nuclear reactor staff for their helpful assistance.

References

[1] S.L. Bellinger, D.S. McGregor, W.J. McNeil, K.A. Nelson, M.F. Ohmes, Gas-filled Neutron Detectors Having Improved Detection Efficiency, US Patent 8519350, 2013.
[2] S.L. Bellinger, D.S. McGregor, K.A. Nelson, Gas-filled Neutron Detectors and Imaging System and Array of Such Detectors, PCT Appln. no., PCT/US2013/0228696, 2013.
[3] K.A. Nelson, S.L. Belling, B.W. Montag, J.L. Neihart, T.A. Riedel, A.J. Schmidt, D.S. McGregor, Nuclear Instruments and Methods A 669 (2012) 79.
[4] K.A. Nelson, S.L. Bellinger, B.W. Montag, J.L. Neihart, T.A. Riedel, A.J. Schmidt, D.S. McGregor, IEEE Transactions on Nuclear Science NS20 (2) (2011) 1026.
[5] N. Tsoulfanidis, Measurement and Detection of Radiation, 2nd edition, Taylor and Francis, New York, 1995.
[6] G.F. Knoll, Radiation Detection and Measurement, 3rd edition, Wiley, New York, 2000.
[7] D.S. McGregor, M.D. Hammig, Y.-H. Yang, H.K. Gersch, R.T. Klann, Nuclear Instruments and Methods A 500 (2003) 272.
[8] L.A. Boatner, J.S. Neal, M.A. Blackston, J.A. Kolopus, J.O. Ramey, Nuclear Instruments and Methods A 693 (2012) 244.
[9] J. Ziegler, J. Biersack, Stopping Ranges of Ions in Matter (SRIM), Version 2008.